Diapycnal mixing in the thermocline: estimates from the C-SOLAS NE Pacific mooring

Philippe Benoit, Eric Kunze and Svein Vagle

School of Earth and Ocean Sciences, University of Victoria, British Columbia, Canada e-mail: pb@uvic.ca

1. Introduction

Air-sea gas exchange is modulated through an O(100 m) oceanic boundary layer, commonly referred to as the surface mixed layer (ML). The effects of physical processes in the upper thermocline (i.e. the tens of meters immediately below the ML, characterized by steep temperature and density gradients) play an important role for the geochemical cycle of carbon and yet are poorly understood[1]. In particular, mixing originating from internal wave fluctuations in this region is often represented as a simple 'background diffusivity' (~ 10^{-4} m^2s^{-1}), constant in time and space.

The Canadian SOLAS NE Pacific mooring at OWS Papa (FIG. 1), active from September 2002 to July 2006, was designed to study air-sea exchange in the oceanic boundary layer for an region subject to high winds and seasonal cycles of vertical stratification. Using the mooring data from the 2005-2006 year, combined with density estimates compiled from Argo[2] floats, we derived estimates of diffusivity (K) below the ML.

Our research look closely at the following topics:

- **What are the temporal and vertical spatial scales of mixing below the ML?**
- **How do these affects the transfer of gases in the upper thermocline?**

This poster looks in details at a small subset of our data.

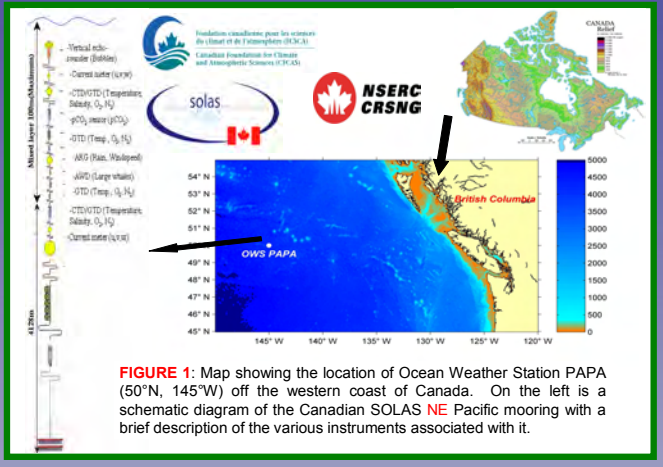

FIGURE 1: Map showing the location of Ocean Weather Station PAPA (50°N, 145°W) off the western coast of Canada. On the left is a schematic diagram of the Canadian SOLAS NE Pacific mooring with a brief description of the various instruments associated with it.

2. Data

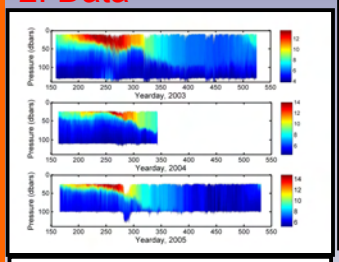

FIGURE 2: Temperature readings with respect to pressure for 3 C-SOLAS measurement years. Note that only 6 months of CTD data were available for the 2004-2005 year.

Temperature readings for the C-SOLAS mooring are shown in FIG. 2. We consider two 10-day periods of the available dataset in 2005; Period 1 (FIG. 3, A to D) from June 15th to the 25th, when the ML depth is shallow at ~30 m; and Period 2 (FIG. 3, E to H) from November 2nd to the 12th, when the ML ends at ~80 m and is progressively deepening. Both periods are strongly influenced by semidiurnal tidal currents.

For both data subsets we plotted the temperatures (with ML depth as a thick black line), velocity shear (V_z), buoyancy frequency (N) and the inverse Richardson number ($Ri^{-1} = V_z^2 / N_2$). The latter highlights the locations of potential dynamic instabilities (i.e. $Ri^{-1} > 4$) beneath the ML.

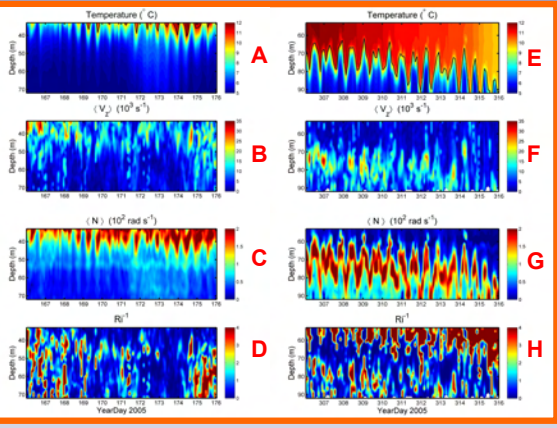

FIGURE 3: Data readings for 2 selected periods of the C-SOLAS 2005 dataset. Period 1 (left plots: days 166-176) and Period 2 (right plots: days 306-316). **A & E**: Temperature (ML depth indicated as black line) **B & F**: Velocity shear **C & G**: Buoyancy frequency **D & H**: inverse Richardson number.

3. Diffusivity estimates

Energy transfer in the oceanic internal wave field shows a net flux towards small spatial scales that increases the shear (V_z) with respect to the stratification (N^2) until wave breaking occurs. If the wave field is varying slowly in time, we can express the turbulent wave breaking dissipation term ε in terms of internal wave parameters[3]. The vertical diffusivity can then be estimated as $K \sim 0.2\ \varepsilon / N^2$.

Using the above equation we computed diffusivities using a shear-dependent dissipation model[4] ($K_{shear} \approx \varepsilon(V_z^4, N^2)$) which has factor of 2 errors. The results from 10-m vertical spatial averaging of both our selected periods are shown in FIG. 4. The steep density gradients and strong shear input from the surface winds result in orders of magnitude variability for K_{shear}.

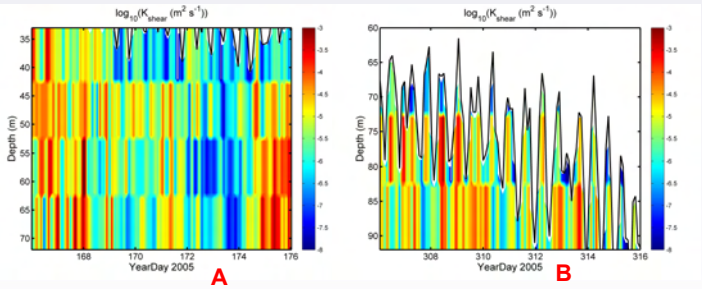

FIGURE 4: $LOG_{10}(K_{shear})$ results for Period 1 (A) and Period 2 (B) of the C-SOLAS 2005 mooring. Thick black lines indicate the position of the ML depth. The ML waters are not suitable for the K parameterization due to their very low stratification.

4. Link to gas data?

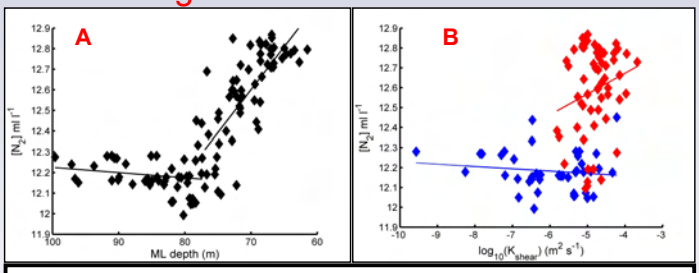

FIGURE 5: A) Scatter plot of ML depths vs nitrogen gas concentration ($[N_2]$) calculated from the 77-m gas-tension device (GTD) for Period 2 B) Scatter plot of the same nitrogen concentration vs. the Kshear average below the ML. Red diamonds represent times when the GTD is beneath the ML, while blue diamonds are times when the GTD is in it. The similar trends between the two plots indicate both gas concentrations and diffusivities are dependent on the ML depth. Low gas concentrations are associated with low diffusivities below the ML

5. Conclusions

- **Though our measurements have considerable uncertainty, our preliminary results indicate that there is extensive variability in the estimated vertical diffusivity inferred from internal wave parameters below the ML, with values ranging several orders of magnitude above and below 10^{-4} m^2s^{-1}.**

- **There is a potential link between the gas concentrations in the ML and the water column diffusivity below it. However, there is limited information available through the data analysis methods we applied. Our next step is to implement a dynamical model of the mixed layer containing the gas tracers(N_2,O_2) measured by the C-SOLAS mooring.**

References

[1] Hamme, R.C. and Emerson, S.R. (2006), Constraining bubble dynamics and mixing with dissolved gases: Implications for productivity measurements by oxygen mass balance, J. Mar. Res., 64, 73-95.

[2] Freeland, H.J. and Cummins, P.F. (2005), Argo: a new tool for environmental assessment and monitoring of the world's oceans. Progress in Oceanography 64, 31-44.

[3] Kunze, E. et al. (2006), Global abyssal mixing inferred from lowered ADCP shear and CTD strain profiles, J. Phys. Oceanogr., 36, 1553-1576.

[4] Gregg, M.C. (1989), Scaling turbulent dissipation in the thermocline, J. Geophys. Res., 94, 9686-9698.

We would also like to thank Nick Hall-Patch and Darren Tuele for their important contributions to this work.